Supporting Information

Electrocatalysis of layered Group 5 metallic transition metal dichalcogenides (MX_2, M= V, Nb, Ta; X=S, Se, Te)

Xinyi Chia,[a] Adriano Ambrosi,[a] Petr Lazar,[b] Zdeněk Sofer[c] Martin Pumera[*a]*

[a] Division of Chemistry & Biological Chemistry, School of Physical and Mathematical Sciences, Nanyang Technological University, Singapore 637371, Singapore.

[b] Regional Centre of Advanced Technologies and Materials, Department of Physical Chemistry, Faculty of Science, Palacký University Olomouc, tř. 17. Listopadu 12, 771 46 Olomouc, Czech Republic.

[c] Department. of Inorganic Chemistry, University of Chemistry and Technology Prague, Technicka 5, 166 28, Prague 6, Czech Republic.

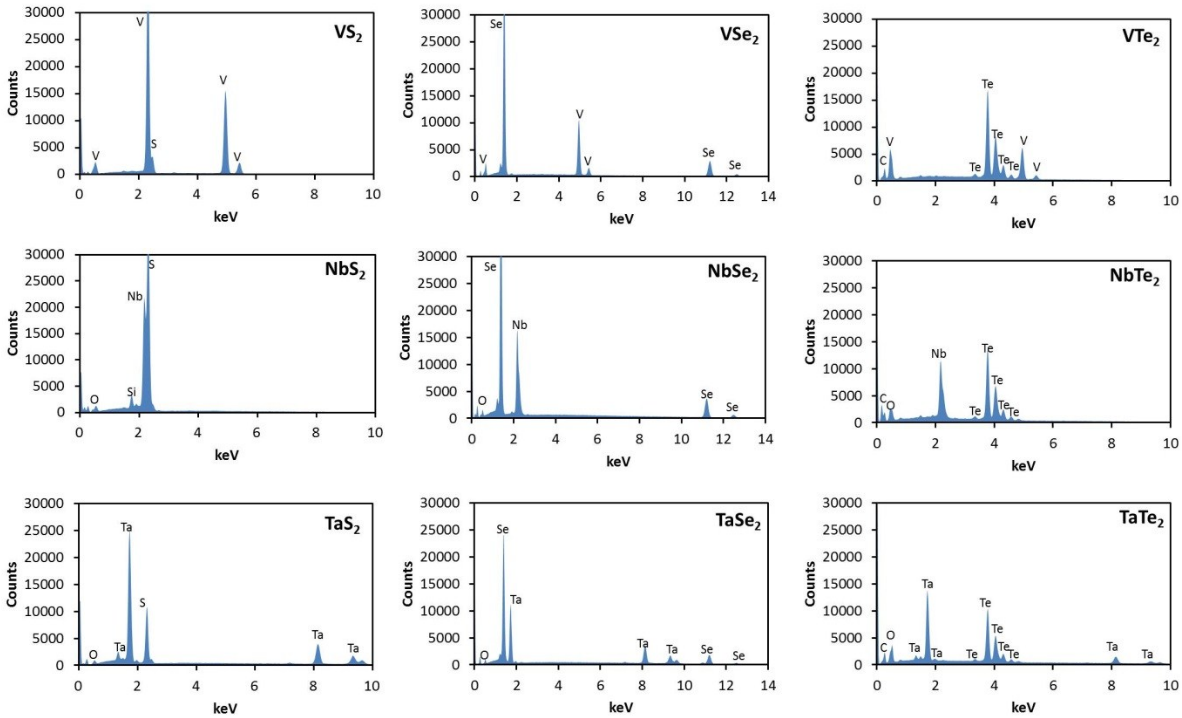

Fig. S1 EDS spectrum of VS_2, VSe_2, VTe_2, NbS_2, $NbSe_2$, $NbTe_2$, TaS_2, $TaSe_2$ and $TaTe_2$.

Table S1 Elemental composition of Group 5 TMDs based on energy-dispersive X-ray spectroscopy.

TMD	V at.%	Nb at. %	Ta at. %	S at. %	Se at. %	Te at. %	C at. %	O at. %	Al at. %	Cl at. %	Si at. %
VS_2	19.55	-	-	33.02	-	-	22.50	24.79	0.15	-	-
VSe_2	14.10	-	-	-	22.65	-	36.94	25.93	-	-	0.39
VTe_2	29.07	-	-	-	-	44.67	25.20	-	0.96	-	-
NbS_2	-	10.77	-	19.53	-	-	60.26	7.74	-	0.19	1.51
$NbSe_2$	-	9.97	-	-	17.08	-	63.30	9.35	-	-	-
$NbTe_2$	-	17.68	-	-	-	32.06	37.90	11.45	0.91	-	-
TaS_2	-	-	13.42	23.53	-	-	53.86	9.19	-	-	-
$TaSe_2$	-	-	9.73	-	17.84	-	61.08	11.35	-	-	-
$TaTe_2$	-	-	12.72	-	-	26.71	35.72	23.89	0.96	-	-

Table S2 Chalcogen-to-metal ratios of Group 5 TMDs based on energy-dispersive X-ray spectroscopy.

Sample	Chalcogen/Metal Ratio
VS_2	1.7
VSe_2	1.6
VTe_2	1.5
NbS_2	1.8
$NbSe_2$	1.7
$NbTe_2$	1.8
TaS_2	1.8
$TaSe_2$	1.8
$TaTe_2$	2.1

Fig. S2 Scanning electron micrographs and corresponding energy-dispersive X-ray maps of the various Group 5 TMDs.

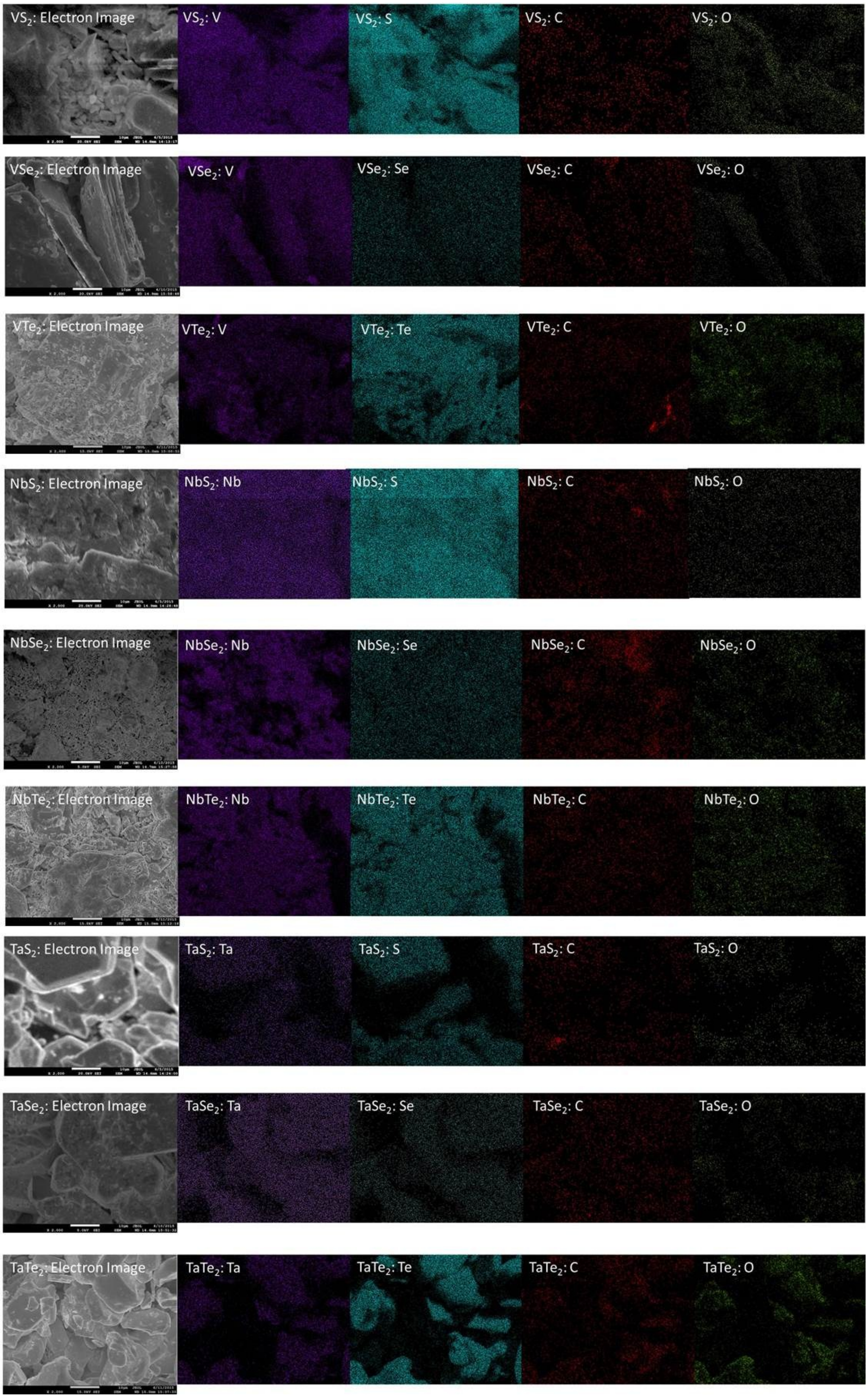

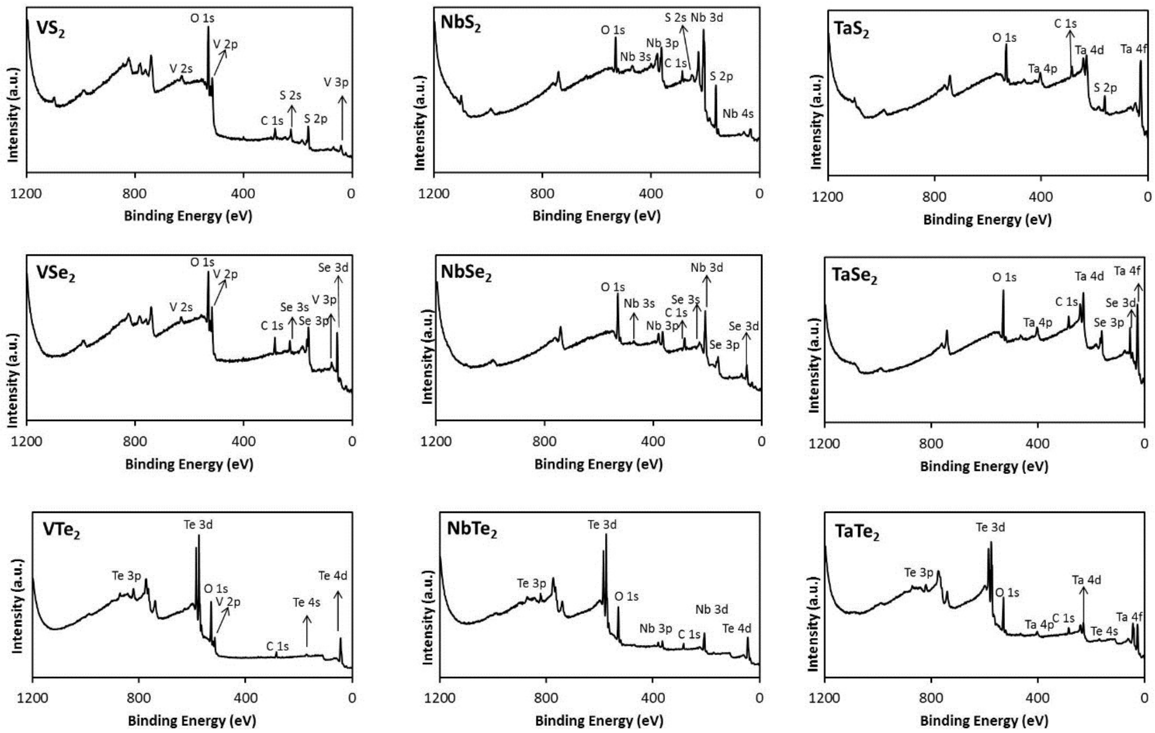

Fig. S3 Wide scan XPS spectra of VS_2, VSe_2, VTe_2, NbS_2, $NbSe_2$, $NbTe_2$, TaS_2, $TaSe_2$ and $TaTe_2$.

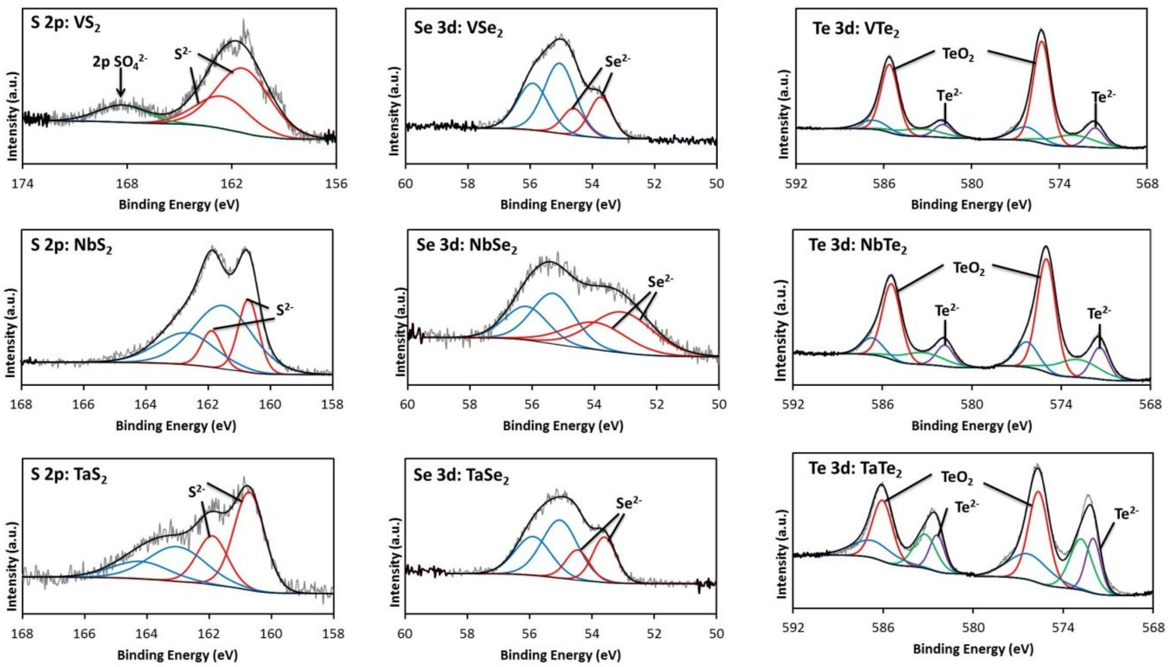

Fig. S4 High resolution X-ray photoelectron spectra of S 2p, Se 3d and Te 3d regions of the Group 5 TMDs. The deconvoluted peaks correspond to the numerous oxidation states of S, Se and Te.

Table S3.1 Tabulated chalcogen-to-metal ratios of VS_2, VSe_2 and VTe_2 based on high resolution X-ray photoelectron spectroscopy, with estimated distributions of the various oxidation states of vanadium after deconvolution of the V 2p peaks.

Sample	V(0)	V(II)	V(III)	V(IV)	V(V)	Chalcogen/Metal Ratio
VS_2	10.0	17.4	10.9	46.6	15.1	1.1
VSe_2	3.4	19.7	16.6	28.1	32.2	1.1
VTe_2	8.2	16.9	18.4	24.4	32.1	2.0

Table S3.2 Tabulated chalcogen-to-metal ratios of NbS_2, $NbSe_2$ and $NbTe_2$ based on high resolution X-ray photoelectron spectroscopy, with estimated distributions of the various oxidation states of niobium after deconvolution of the high resolution Nb 3d peaks.

Sample	Nb(0)	Nb(I)	Nb(II)	Nb(IV)	Nb(V)	Chalcogen/Metal Ratio
NbS_2	1.5	16.5	40.0	18.8	23.2	1.6
$NbSe_2$	4.7	0.1	3.7	32.3	59.2	0.9
$NbTe_2$	4.5	2.8	7.5	44.9	40.3	3.0

Table S3.3 Tabulated chalcogen-to-metal ratios of TaS_2, $TaSe_2$ and $TaTe_2$ based on high resolution X-ray photoelectron spectroscopy, with estimated distributions of the various oxidation states of tantalum after deconvolution of the high resolution Ta 4f peaks.

Sample	Ta(0)	Ta(I)	Ta(II)	Ta(IV)	Ta(V)	Chalcogen/Metal Ratio
TaS_2	1.0	16.1	14.7	40.2	28.0	1.1
$TaSe_2$	2.1	12.0	9.8	63.8	12.3	1.0
$TaTe_2$	1.5	9.5	1.8	64.0	23.2	2.6

Table S4 Estimated distributions of the various oxidation states of vanadium after deconvolution of the high resolution V 2p peaks and O 1s peaks based on XPS.

Sample	V(0)	V(II)	V(III)	V(IV)	V(V)	O 1s
VS_2	4.2	7.4	4.6	19.9	6.5	57.4
VSe_2	1.4	7.8	6.6	11.2	12.9	60.1
VTe_2	2.8	5.8	6.3	8.3	10.9	65.9

Table S5 Elemental compositions Group 5 TMDs based on wide-scan X-ray photoelectron spectroscopy.

Sample	V 2p	Nb 3d	Ta 4f	S 2p	Se 3d	Te 3d	C 1s	O 1s
VS_2	6.2	-	-	29.9	-	-	27.6	36.3
VSe_2	3.3	-	-	-	30.4	-	35.8	30.5
VTe_2	1.1	-	-	-	-	14.2	30.4	54.3
NbS_2	-	24.3	-	37.2	-	-	15.5	23.0
$NbSe_2$	-	19.1	-	-	19.0	-	24.8	37.1
$NbTe_2$	-	10.3	-	-	-	10.3	56.4	23.0
TaS_2	-	-	20.8	18.0	-	-	29.4	31.8
$TaSe_2$	-	-	18.5	-	18.5	-	27.7	35.3
$TaTe_2$	-	-	13.6	-	-	10.7	27.0	48.7

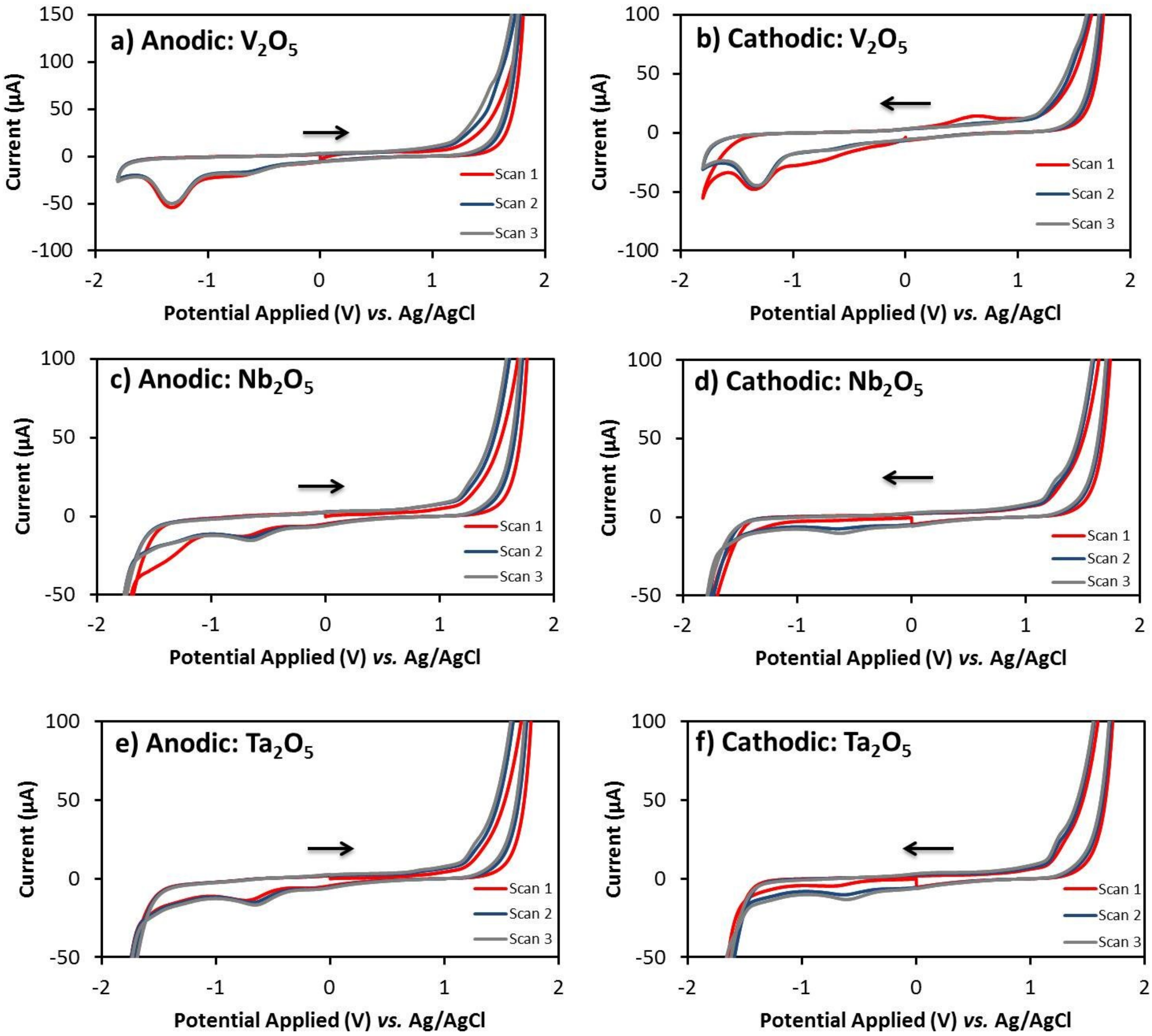

Fig. S5 Cyclic voltammograms of a) V_2O_5 during anodic scan and b) cathodic scan, c) Nb_2O_5 during anodic scan and d) cathodic scan, e) Ta_2O_5 during anodic scan and f) cathodic scan. Conditions: background electrolyte PBS (50 mM) pH 7.0; scan rate, 100 mV s^{-1}; scans begin at 0.0 V *vs.* Ag/AgCl. The arrows denote initial scan direction.

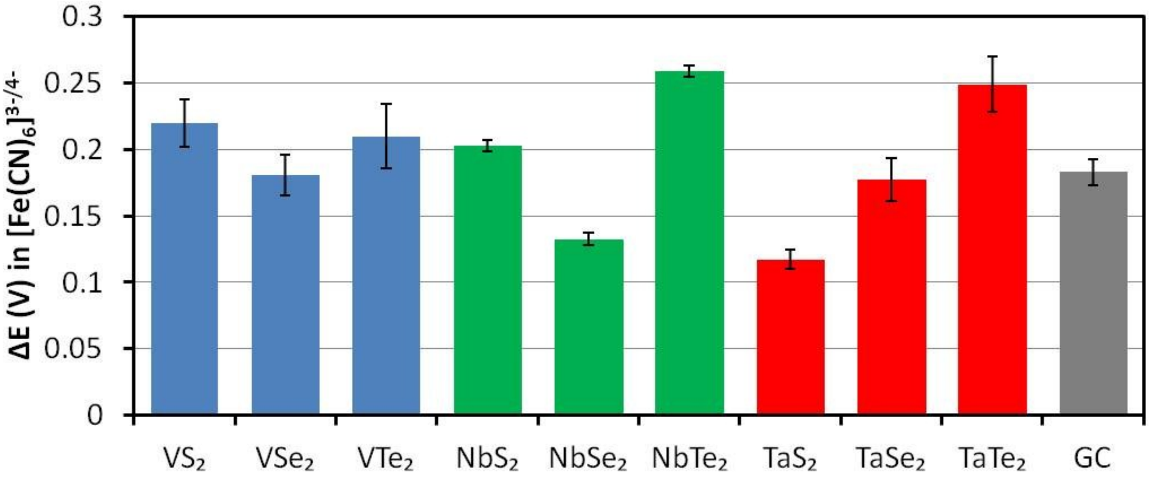

Fig. S6 Summary of peak-to-peak separations of all Group 5 TMDs with their corresponding error bars. Conditions: background electrolyte, KCl (0.1 M); scan rate, 100 mV s^{-1}; all measurements are performed relative to Ag/AgCl reference electrode.

Table S6 Table of heterogeneous electron transfer (HET) rate constant, k^0_{obs}, for all the Group 5 TMDs. The k^0_{obs} of the bare glassy carbon electrode is also computed as a basis for comparison.

Material	k^0_{obs} (cm s^{-1})
VS_2	8.41×10^{-4}
VSe_2	1.43×10^{-3}
VTe_2	9.61×10^{-4}
NbS_2	1.06×10^{-3}
$NbSe_2$	2.75×10^{-3}
$NbTe_2$	4.95×10^{-4}
TaS_2	3.39×10^{-3}
$TaSe_2$	1.50×10^{-3}
$TaTe_2$	5.65×10^{-4}
GC	1.29×10^{-3}

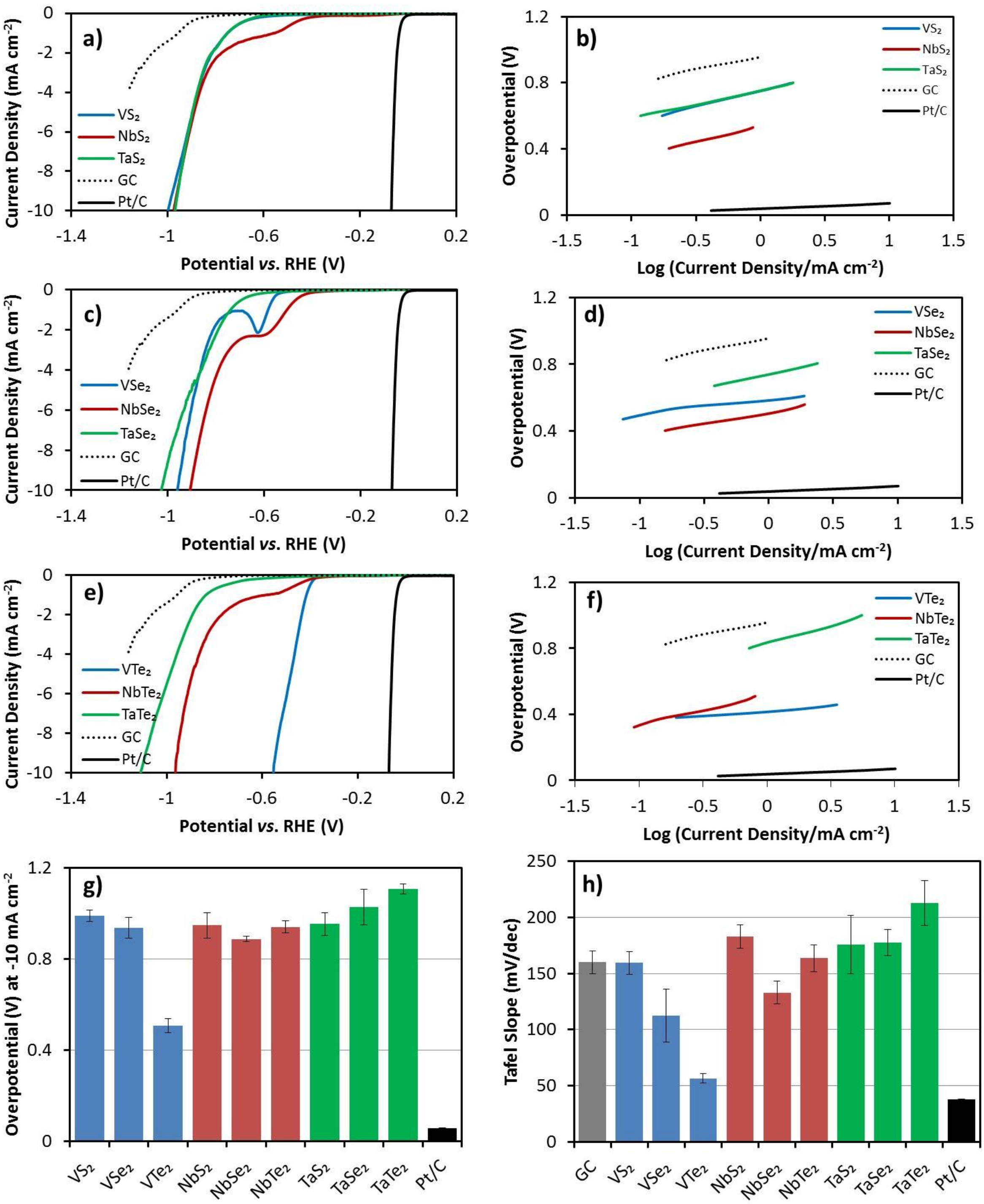

Fig. S7 Linear sweep profiles of hydrogen evolution reaction (HER) on GC electrodes modified with a) VS_2, NbS_2 and TaS_2, c) VSe_2, $NbSe_2$ and $TaSe_2$ and e) VTe_2, $NbTe_2$ and $TaTe_2$. Tafel plots for HER corresponding to b) VS_2, NbS_2 and TaS_2, d) VSe_2, $NbSe_2$ and $TaSe_2$ and f) VTe_2, $NbTe_2$ and $TaTe_2$. Histograms summarize the averages of g) HER overpotential at current density of -10 mA cm^{-2} and h) Tafel slopes for all the materials. Conditions: background electrolyte, H_2SO_4 (0.5 M); scan rate, 2 mV s^{-1}.

Table S7 Table of exchange current density, *j*, for all the Group 5 TMDs. The *j* of the Pt/C is also computed as a basis for comparison.

Material	***j* (mA cm^{-2})**
VS_2	3.80×10^{-5}
VSe_2	1.89×10^{-5}
VTe_2	1.83×10^{-7}
NbS_2	1.20×10^{-3}
$NbSe_2$	9.03×10^{-5}
$NbTe_2$	7.90×10^{-4}
TaS_2	1.71×10^{-4}
$TaSe_2$	1.78×10^{-5}
$TaTe_2$	1.47×10^{-4}
Pt/C	6.20×10^{-2}

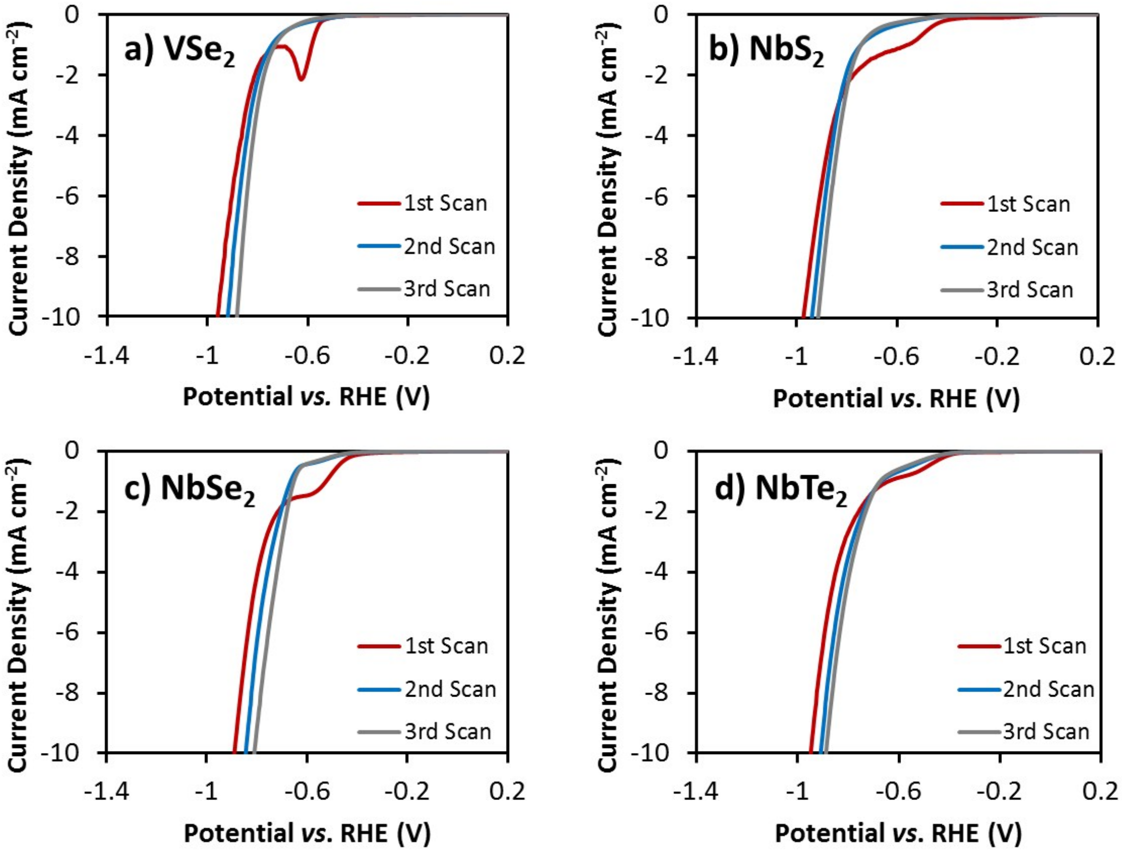

Fig. S8 Polarisation curves demonstrating the effect of subsequent scans on the HER pre-waves of a) VSe_2, b) NbS_2, c) $NbSe_2$ and d) $NbTe_2$. Conditions: background electrolyte, H_2SO_4 (0.5 M); scan rate, 2 mV s^{-1}.

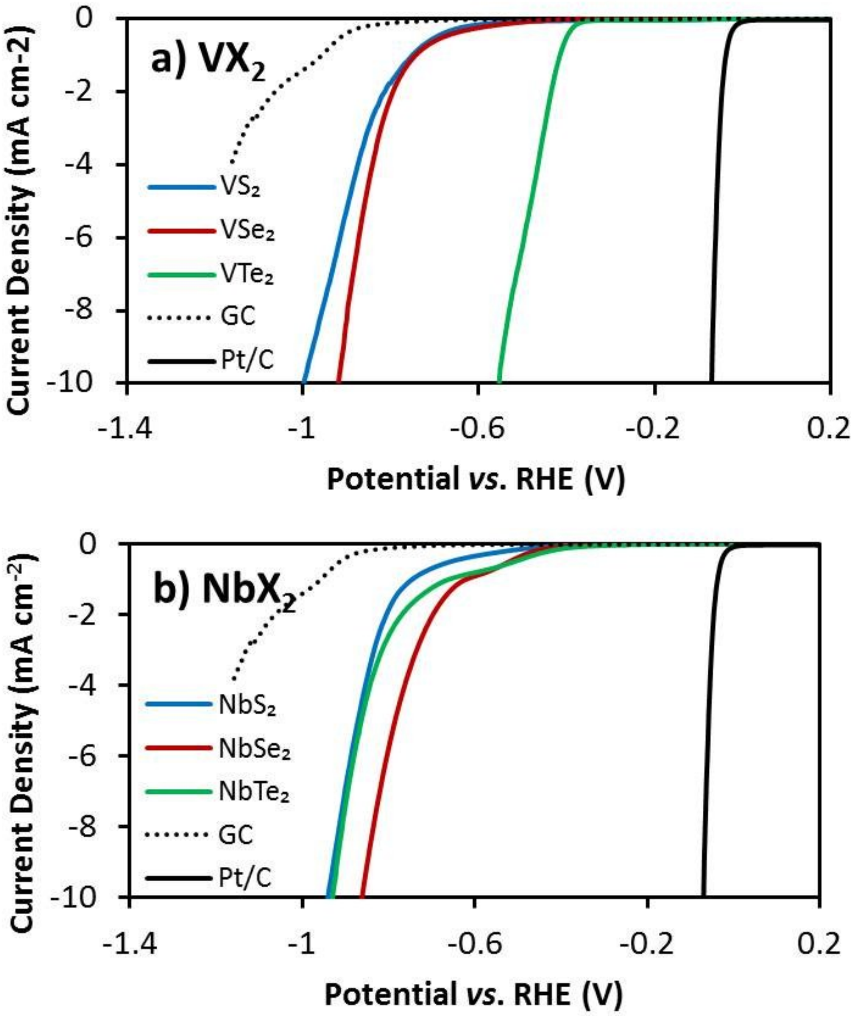

Fig. S9 Polarisation curves demonstrating the effect of subsequent scans with the absent or diminished HER pre-wave on the HER trends of Group 5 TMDs. Linear sweep profiles of hydrogen evolution reaction (HER) on GC electrodes modified with a) VS_2, VSe_2 and VTe_2 and b) NbS_2, $NbSe_2$ and $NbTe_2$. All Group 5 TMDs shown are first scans with the exception of VSe_2, NbS_2, $NbSe_2$ and $NbTe_2$ whereby their 2^{nd} scans are used. Conditions: background electrolyte, H_2SO_4 (0.5 M); scan rate, 2 mV s^{-1}.

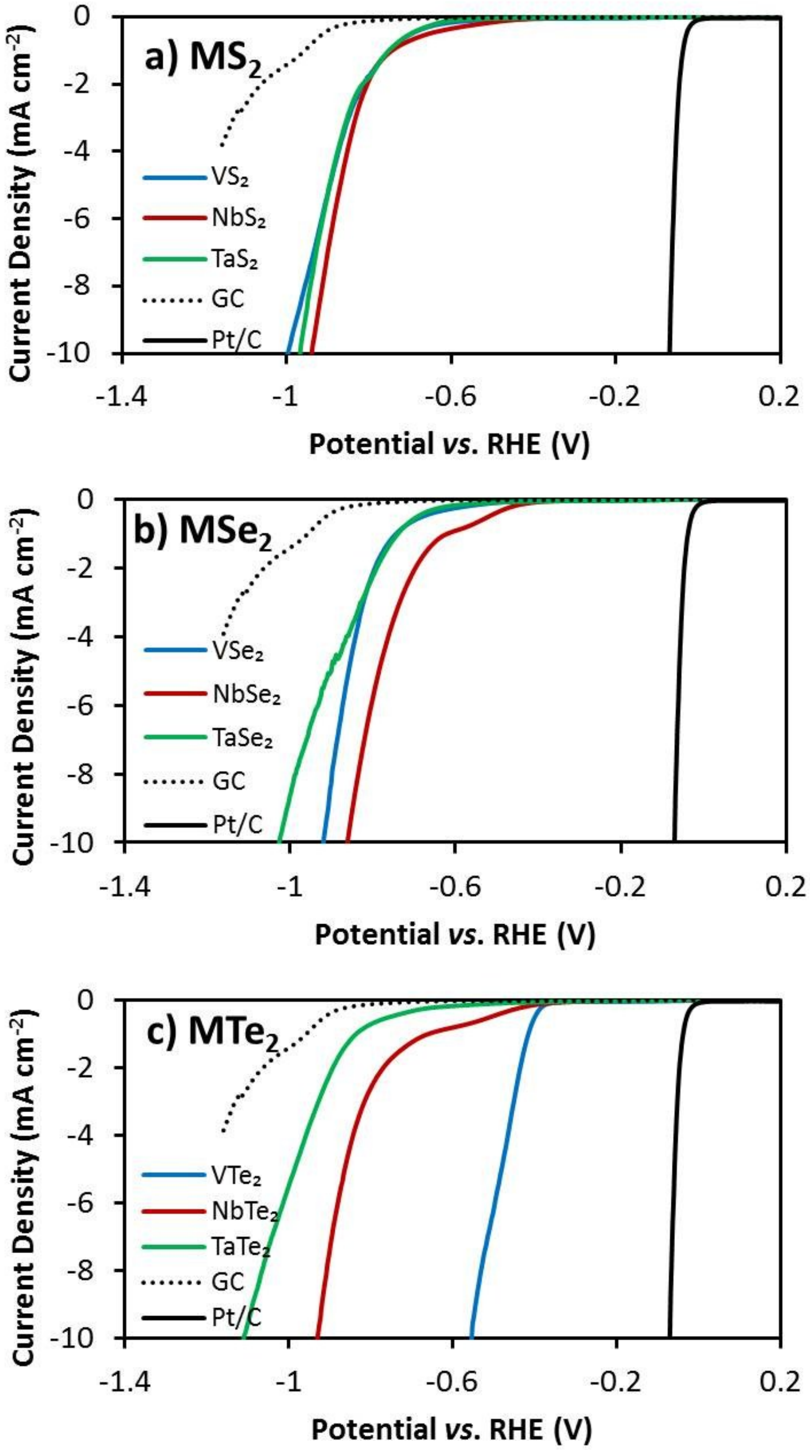

Fig. S10 Polarisation curves demonstrating the effect of subsequent scans with the absent or diminished HER pre-wave on the HER trends of Group 5 TMDs. Linear sweep profiles of hydrogen evolution reaction (HER) on GC electrodes modified with a) VS_2, NbS_2 and TaS_2, b) VSe_2, $NbSe_2$ and $TaSe_2$ and c) VTe_2, $NbTe_2$ and $TaTe_2$. All Group 5 TMDs shown are first scans with the exception of VSe_2, NbS_2, $NbSe_2$ and $NbTe_2$ whereby their 2nd scans are used. Conditions: background electrolyte, H_2SO_4 (0.5 M); scan rate, 2 mV s^{-1}.

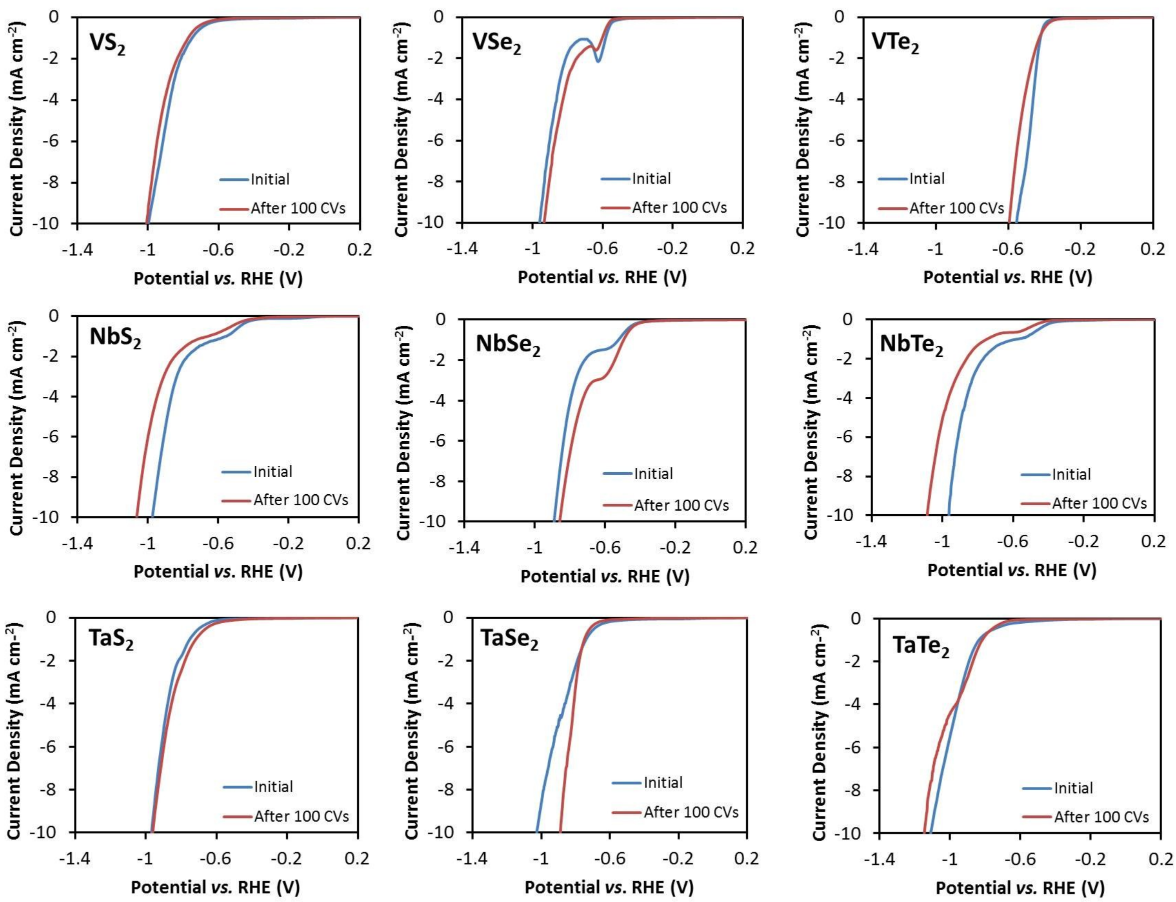

Fig. S11 HER polarisation curves of all Group 5 TMDs before and after 100 cyclic voltammetry cycles in sulfuric acid. Conditions: background electrolyte, H_2SO_4 (0.5 M); scan rate, 2 mV s^{-1}.

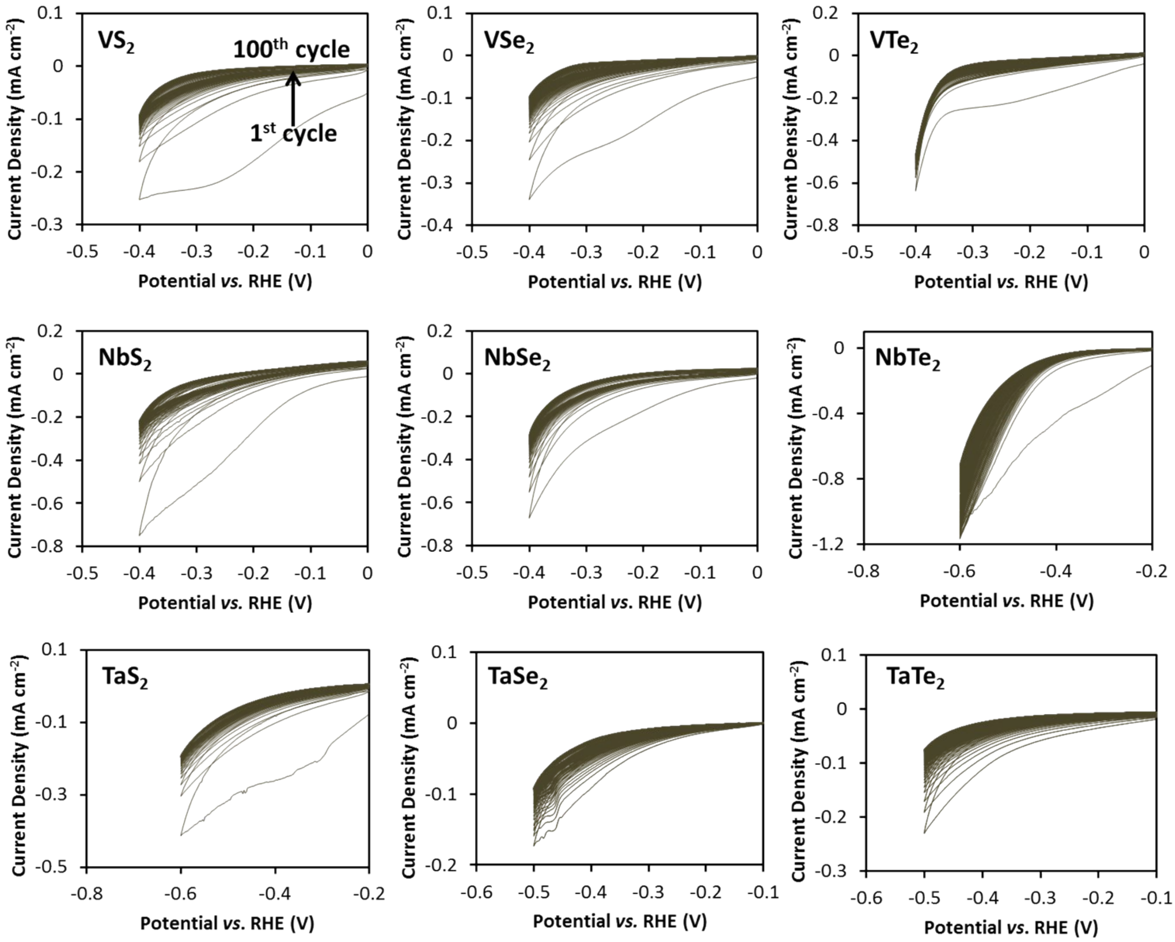

Fig. S12 Cyclic voltammograms of all Group 5 TMDs to examine catalytic stability in acid. Conditions: background electrolyte, H_2SO_4 (0.5 M); scan rate, 100 mV s^{-1}.

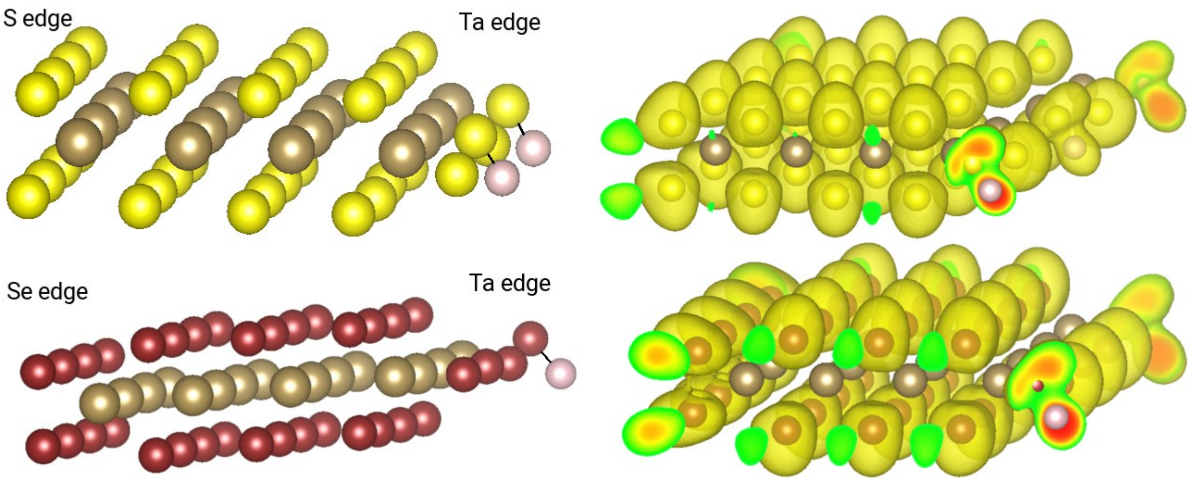

Fig. S13 The geometry (left panels) of the two hydrogen atoms (in violet) adsorbed on the Ta-edge of TaS_2 (upper panel), and single hydrogen atom adsorbed on the Ta-edge of $TaSe_2$. The panels on the right panels show the electron localization function (ELF) of respective geometry and the ELFs are cut through S-H and Se-H bond.

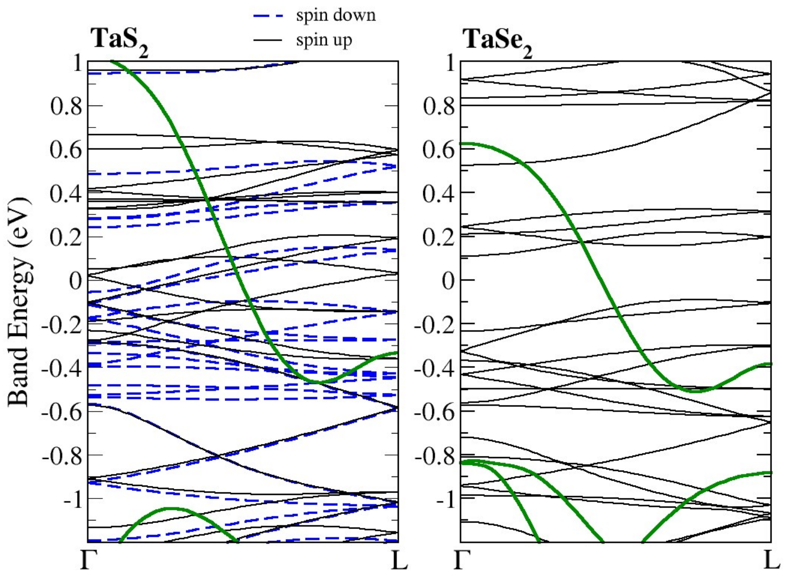

Fig. S14 The electronic band-structure of the TaS_2 nanowire (left) and the $TaSe_2$ nanowire (right). The nanowire exposes both the Ta-edge and the S-edge. The TaS_2 nanowire becomes spin-polarized, whereas $TaSe_2$ is nonmagnetic. The green lines show the band structure of single-layer TaS_2 and $TaSe_2$ (without any edge).